Impact of episodic vertical fluxes on sea surface pCO $_2$

A. Mahadevan, A. Tagliabue, L. Bopp, A. Lenton, L. Mémery and M. Lévy

References	**This article cites 35 articles, 1 of which can be accessed free** http://rsta.royalsocietypublishing.org/content/369/1943/2009.full.html#ref-list-1
Rapid response	Respond to this article http://rsta.royalsocietypublishing.org/letters/submit/roypta;369/1943/2009
Subject collections	Articles on similar topics can be found in the following collections oceanography (32 articles) climatology (98 articles)
Email alerting service	Receive free email alerts when new articles cite this article - sign up in the box at the top right-hand corner of the article or click **here**

Impact of episodic vertical fluxes on sea surface pCO_2

By A. Mahadevan[1], A. Tagliabue[2], L. Bopp[2], A. Lenton[3], L. Mémery[4] and M. Lévy[5],*

[1] *Department of Earth Sciences, Boston University, Boston, MA, USA*
[2] *Laboratoire des Sciences du Climat et de l'Environnement, IPSL/CEA/CNRS/UVSQ, Orme des Merisiers, 91198 Gif-sur-Yvette, France*
[3] *CSIRO Wealth from Oceans National Research Flagship, Hobart, Tasmania, Australia*
[4] *LEMAR, UBO/CNRS/IRD, Institut Universitaire Européen de la Mer (IUEM), Technopole Brest Iroise, 29280 Plouzané, France*
[5] *LOCEAN-IPSL, CNRS/UPMC/IRD, 4 place Jussieu, 75252 Paris Cedex 05, France*

Episodic events like hurricanes, storms and frontal- and eddy-driven upwelling can alter the partial pressure of CO_2 (pCO_2) at the sea surface by entraining subsurface waters into the surface mixed layer (ML) of the ocean. Since pCO_2 is a function of total dissolved inorganic carbon (DIC), temperature (T), salinity and alkalinity, it responds to the combined impacts of physical, chemical and biological changes. Here, we present an analytical framework for assessing the relative magnitude and sign in the short-term perturbation of surface pCO_2 arising from vertical mixing events. Using global, monthly, climatological datasets, we assess the individual, as well as integrated, contribution of various properties to surface pCO_2 in response to episodic mixing. The response depends on the relative vertical gradients of properties beneath the ML. Many areas of the ocean exhibit very little sensitivity to mixing owing to the compensatory effects of DIC and T on pCO_2, whereas others, such as the eastern upwelling margins, have the potential to generate large positive/negative anomalies in surface pCO_2. The response varies seasonally and spatially and becomes more intense in subtropical and subpolar regions during summer. Regions showing a greater pCO_2 response to vertical mixing are likely to exhibit higher spatial variability in surface pCO_2 on time scales of days.

Keywords: CO_2; oceanic pCO_2; dissolved inorganic carbon; sea-surface variability; vertical mixing

*Author for correspondence (marina.levy@upmc.fr).

1. Introduction

The ocean plays a critical role in mitigating climate change taking up nearly 30 per cent of anthropogenic CO_2 emissions [1]. The air–sea flux of CO_2 depends on the difference in the partial pressures of CO_2 (pCO_2) between the atmosphere and sea surface, as well as wind speed and air–sea interfacial conditions (e.g. [2]). Oceanic surface pCO_2 is a function of dissolved inorganic carbon (DIC), temperature (T), salinity (S) and alkalinity (ALK). Hence, it responds to physical processes, such as mixing, deep convection and water mass transformation, as well as biological processes like net primary production (NPP) and remineralization of organic matter. Each of the drivers of oceanic pCO_2 has its own temporal and spatial scales of response to dynamical change. Unsurprisingly, surface pCO_2 is highly variable in space and time, and much of the variability occurs on short time scales [3]. Global studies have focused on understanding the large-scale, seasonal patterns in sea-surface pCO_2 and in quantifying the related air–sea fluxes of CO_2 at coarse spatial and temporal resolution ($4° \times 5°$ monthly) [4]. On the other hand, disparate findings have been reported about the variability and controlling factors of surface pCO_2 on short space and time scales [5–11], suggesting that there is clearly need for a unified, mechanistic understanding of how surface pCO_2 responds to episodic, localized events that induce vertical mixing.

While the surface layer of the ocean is fairly well mixed, there are strong gradients in the vertical distribution of properties beneath the mixed layer (ML). With increasing depth, T decreases, DIC, S and nutrients increase, whereas ALK can increase or decrease depending on the depth and location. Therefore, any physical process that generates localized overturning, up-/downwelling or diapcynal mixing, and entrains water from below the ML, can change the physical–chemical properties in the surface ML. This, along with any subsequent biological changes in response to it, can significantly perturb the mean state of surface pCO_2. We will refer to processes that lead to a vertical flux of properties across the base of the ML, more generally, as 'mixing'. Potential mechanisms that can induce such events include negative buoyancy fluxes causing convection, frontal dynamics [12,13], localized upwelling/mixing owing to wind variability [14], storms and hurricanes [15], and proposed geo-engineering schemes such as ocean pipes [16]. Indeed, the importance of such vertical mixing events on phytoplankton production and the biological pump is now widely recognized [17–21]. However, their effect on surface pCO_2 is more complex and difficult to generalize owing to the multiple factors that control pCO_2.

Several regional studies have examined the short-term response of sea-surface pCO_2 to mixing events. Modelling studies of the eastern North Atlantic found little or no change in the surface pCO_2 in response to upwelling induced by fronts and eddies because additional DIC was counterbalanced by reduced temperature [22,23]. Perrie *et al.* [24] and Bates *et al.* [15] reported opposing changes in surface pCO_2 in response to hurricane events. These studies highlight the complex interactions of the drivers of oceanic pCO_2 and the difficulty in generalizing the response globally. While global modelling studies [25,26] that evaluated the ocean pipe geo-engineering schemes

examine biological and physical changes owing to vertical fluxes, these studies focused on the longer term impacts through the implementation of a quasi-permanent perturbation to the system. Nevertheless, they also highlight the high degree of spatial variability in the biological and physical response to vertical fluxes.

In this study, we develop a general theoretical framework, accounting for physical and biological changes in response to mixing, such that the modulation of surface pCO_2 by individual properties, as well as their integrated effect, can be understood on short time scales. The magnitude of the response depends not only on the intensity and duration of the mixing, but also on the location and timing of the events. We quantify the response of surface pCO_2 in terms of the contributions from changes in DIC, T, S and ALK. The sum of these changes can act to either increase or decrease pCO_2. We evaluate these contributions and their integral effect using climatological observations of T, DIC, ALK, nitrate (NO_3) and S. In this study, we apply our framework for assessing short-term perturbations from the monthly, mean and climatological distributions. It is complementary to studies of climatological, monthly pCO_2 variability that include the large-scale longer term response but ignore the short spatial and temporal scale response. It provides a context and mechanistic framework in which differing regional responses can be interpreted. But, the method may also be used with other observational data to examine perturbations arising from specific events on a regional scale.

The theoretical framework we present here addresses time scales representative of events lasting up to a few days. We neglect the air–sea exchange of heat, freshwater and CO_2 in our calculations. Horizontal transport is neglected and only vertical fluxes owing to various processes (advective and diapycnal) are represented through a vertical eddy diffusivity acting at the base of the ML. For the sake of this analysis, the mixed layer depth (MLD) and vertical profiles of the oceanic properties (T, DIC, ALK, NO_3) are assumed not to be modified by the vertical mixing. Redfield ratios are used to estimate biological uptake of DIC, and only NO_3 is considered as a limiting nutrient (e.g. iron or silicate limitation is neglected). Our analysis relies on using modern climatologies (World Ocean Atlas 2005 and GLODAP) of temperature [27], salinity [28], NO_3 [29], DIC and ALK [30]. We realize that these datasets are based on sparse measurements; they may not be reliable in some regions such as the Southern Ocean and do not resolve the seasonal variability in DIC and ALK. Our approach is to apply the proposed framework to the best available global datasets in the hope that the broad conclusions are qualitatively correct and will be tested with better datasets in the future. In applying the approach to these datasets, we assume that these large-scale properties are not changing with time, apart from changes owing to the seasonal cycle that are explicitly or implicitly taken into account in our study. Thus our results only apply for the modern state and ignore inter-annual/decadal variability of ocean properties as well as any long-term trends in those properties. Any long-term changes in mixing or property sources/sinks would alter mean distributions and also bring into effect air–sea fluxes and horizontal circulation. Thus, our analysis applies to episodic mixing.

2. Theoretical framework

To quantify the effect of localized upwelling or vertical mixing on surface pCO_2, we express the rate of change of pCO_2 in terms of the various properties on which it is dependent [31] as follows:

$$\frac{\partial pCO_2}{\partial t} = \frac{\partial pCO_2}{\partial T}\frac{\partial T}{\partial t} + \frac{\partial pCO_2}{\partial DIC}\frac{\partial DIC}{\partial t} + \frac{\partial pCO_2}{\partial ALK}\frac{\partial ALK}{\partial t} + \frac{\partial pCO_2}{\partial S}\frac{\partial S}{\partial t}. \quad (2.1)$$

In order to consider the response of the surface ML to small-scale upwelling and/or mixing, we model the vertical flux of any property χ as a diffusive flux described by $\kappa(\partial\chi/\partial z)$, where κ denotes the vertical eddy diffusivity of the property. This is meant to account for mixing, as well as localized vertical advective fluxes that occur at horizontal scales much smaller than the resolution of our datasets (nominally $1° \times 1°$). We, therefore, assume the value of κ to be the same for all the properties. The rate of change in any property χ within the ML of depth H is modelled as

$$\frac{\partial\chi}{\partial t} = -\frac{1}{H}\,\kappa\,\frac{\partial\chi}{\partial z}\bigg|_{z=-H} + S_\chi. \quad (2.2)$$

Here, we consider only a one-dimensional budget for χ to evaluate the effects of vertical mixing/upwelling. The property χ is assumed to be uniformly mixed within the ML and any sources/sinks that alter the property in the ML (other than air–sea fluxes) are denoted by S_χ. Further, $\partial\chi/\partial z|_{z=-H}$ is the vertical gradient across the base of the ML ($z=-H$) that results in a vertical flux into the ML.

We note that the Revelle factors for DIC and ALK, namely

$$\left.\begin{aligned} \xi &= \frac{\Delta pCO_2}{pCO_2}\bigg/\frac{\Delta DIC}{DIC}\bigg|_{ALK=const.} \\ \text{and} \qquad \xi_A &= \frac{\Delta pCO_2}{pCO_2}\bigg/\frac{\Delta ALK}{ALK}\bigg|_{DIC=const.} \end{aligned}\right\} \quad (2.3)$$

are variable in space and time with typical values in the range 8–15 for ξ, and -8 to -13 for ξ_A [32]. For the salinity and temperature range of the ocean, there is a well-established relationship between pCO_2 and T, as well as S [31]:

$$\left.\begin{aligned} \beta &= \frac{1}{pCO_2}\frac{\partial pCO_2}{\partial T} = 0.0423\,°C^{-1} \\ \text{and} \qquad \beta_S &= \frac{1}{pCO_2}\frac{\partial pCO_2}{\partial S} = 0.9^{-1}. \end{aligned}\right\} \quad (2.4)$$

To evaluate the relative change in surface pCO_2 in response to vertical fluxes, we divide both sides of equation (2.1) by the value of pCO_2 in the surface layer. Using equation (2.2) along with the relationships (2.3) and (2.4), and expressing the time rate of change of pCO_2 as $\Delta pCO_2/\Delta t$ we can rewrite equation (2.1) as

$$\frac{\Delta pCO_2}{pCO_2} = -\frac{\kappa\,\Delta t}{H}\left(\beta\frac{\partial T}{\partial z} + \frac{\xi}{DIC}\frac{\partial DIC}{\partial z} + \frac{\xi_A}{ALK}\frac{\partial ALK}{\partial z} + \beta_S\frac{\partial S}{\partial z}\right)$$

$$+ S_T + S_{DIC} + S_{ALK} + S_S. \quad (2.5)$$

This equation describes the relative change in surface pCO_2 arising from the individual responses of DIC, ALK, T and S to vertical mixing across the base of the ML. All values, other than the gradients, are determined in the ML. The first four parenthesized terms on the right-hand side of equation (2.5) denote the relative change in pCO_2 owing to the vertical mixing of T, DIC, ALK and S, whereas the next four terms denote the relative pCO_2 change owing to sources and sinks for T, DIC, ALK and S. We consider perturbations to the surface pCO_2 owing to vertical oceanic transport alone, while neglecting the atmospheric response, i.e. air–sea fluxes in response to the altered surface pCO_2. In other words, we consider the perturbation in surface pCO_2 owing to episodic oceanic processes, but not the consequent air–sea equilibration that is expected to occur on longer time scales (weeks to months) towards neutralizing such perturbations. Surface fluxes of heat, freshwater and CO_2 are therefore not included. Thus, $S_T = S_S = 0$ and S_{DIC} and S_{ALK} account for biological effects. More precisely, S_{DIC} accounts for the uptake of DIC by biological consumption. Vertical mixing and advection supply remineralized nutrients to the surface ocean and stimulate NPP. Since NPP is limited by NO_3 in much of the ocean, we calculate the maximum potential consumption of DIC during NPP by multiplying the NO_3 supplied through vertical mixing with the Redfield C/N ratio, $R_{C:N} = 6.625$. To account for light limitation associated with deepened MLs, we multiply the potential DIC consumption by a light limitation factor $L = 1 - \exp(-(E/E_k))$ that varies between 0 and 1 depending on the mean light availability over the ML. Here E is the climatological ML average of photosynthetically available radiation (PAR) and E_k is a light limitation constant taken to be 80 microeinsteins $m^{-2}\,s^{-1}$. The relative change in pCO_2 owing to the biological consumption of DIC is thus modelled as

$$S_{DIC} = -\frac{\kappa \Delta t}{H}\left(\frac{\xi}{DIC} R_{C:N} L \frac{\partial NO_3}{\partial z}\right). \qquad (2.6)$$

The NO_3 that is supplied by mixing, but is left unconsumed by NPP owing to light limitation, contributes alkalinity, which results in a relative change in pCO_2 calculated as

$$S_{ALK} = \frac{\kappa \Delta t}{H}\left(\frac{\xi_A}{ALK} \frac{\partial NO_3}{\partial z}(1 - L)\right). \qquad (2.7)$$

For much of the ocean, it is reasonable to assume that NO_3 limits biological production. However, in the high-nutrient low-chlorophyll regions of the world's oceans (primarily the Southern, sub-Arctic Pacific and equatorial Pacific Oceans), the micronutrient iron limits biological productivity. Taking into account the limitation of iron or other potentially limiting nutrients like phosphate or silicic acid requires knowledge of that nutrient's distribution and the nutrient-specific limitation in phytoplankton production at each location, which we lack and thus do not include. Similarly, potential changes in species composition and alkalinity consumption during calcification or bacterial remineralization are not accounted for in this study.

3. Datasets and methods

We use a number of different global climatological datasets to evaluate the various terms in equation (2.5), which define the contribution of mixing of individual properties to the relative change in surface pCO_2. MLD, H, based on the fixed density criterion of $0.03\,\text{kg m}^{-3}$ is taken from the monthly climatology of de Boyer Montégut *et al.* [33]. To facilitate a common analysis, we interpolate all the data on to the $1° \times 1°$ grid used in the Global Ocean Data Analysis Project (GLODAP). The GLODAP database [30] provides an annual mean distribution of DIC and ALK mapped on a $1° \times 1°$ grid globally, though it should be remembered that the average spacing between the cruises that make up the GLODAP data often exceeds $10°$. To account for the seasonality in surface DIC and ALK arising from MLD variations, we average the GLODAP values within the ML, whose depth varies from month to month. This gives us a monthly, ML DIC and ALK distribution, which includes seasonality in the MLD, but does not include effects arising from seasonality in biological production and consumption. Such an approach is justified because the removal of DIC by biology contributes only a very small perturbation to the total DIC and its mean profile. Furthermore, a comparison between these monthly DIC and ALK fields estimated for the ML and monthly surface DIC and ALK computed from the surface pCO_2 climatology [4] using an empirical computation of salinity and carbon chemistry [34] reveals that the differences are insignificant for the purposes of this study.

We use monthly values of PAR from the SeaWiFS climatology calculated over the period 1997–1998 to 2009 (http://oceancolor.gsfc.nasa.gov/cgi/l3). These $8\,\text{km} \times 8\,\text{km}$ resolution monthly data are averaged onto the $1° \times 1°$ grid used in this study. To account for the small biological response of the austral and boreal winters, we set the missing values to be $1.25\,\text{einsteins m}^{-2}\,\text{d}^{-1}$. We include the effect of albedo on PAR by using the monthly mean fractional sea ice cover and assuming that when sea ice cover exceeds 50 per cent, PAR is reduced by a factor of 0.5. Our value of 0.5 accounts for the combined albedos of open ocean (0.1), sea ice (0.5–0.7) and snow-covered sea ice (0.8–0.9). Climatological values of sea ice are from Walsh [35] and Zwally *et al.* [36]. We estimate an average value of PAR for the ML using Beer's law for type 1 waters [37] with an e-folding depth scale of 23 m for the attenuation of light downward from the surface.

Monthly temperature [27], salinity [28] and NO_3 [29] are obtained from the World Ocean Atlas (WOA05) and regridded onto the GLODAP grid. We average these fields within the ML for each month to obtain a uniform ML value that we use for consistency with the DIC and ALK fields.

To convert the change in DIC and ALK to pCO_2, we use the approximate empirical relationships for Revelle factors of ALK and DIC following Sarmiento & Gruber [32]: $\xi = (3 \cdot \text{ALK} \cdot \text{DIC} - 2 \cdot \text{DIC}^2)/((2 \cdot \text{DIC} - \text{ALK}) \cdot (\text{ALK} - \text{DIC}))$; $\xi_A = \text{ALK}^2/((2 \cdot \text{DIC} - \text{ALK})(\text{ALK} - \text{DIC}))$. We calculate these values monthly to account for seasonal changes in surface DIC and ALK.

The vertical gradients of properties at the base of the ML are derived by differencing the ML value of the property (obtained as described above) with the value just beneath the ML on the GLODAP grid. Since MLD varies from month to month, so do the gradients at the base of the MLD. The evaluation of vertical gradients in this manner neglects perturbations to the MLD arising from the localized mixing/upwelling events.

In order to compare the relative effects of T, DIC, ALK and the biological uptake of DIC for a given strength of vertical mixing or upwelling (characterized by κ) occurring over a time scale representative of synoptic events, we choose $\kappa = 10^{-3}\,\mathrm{m^2\,s^{-1}}$ and $\Delta t = 1$ day in evaluating each of the terms in equation (2.5). Here, κ represents the vertical eddy diffusivity at the base of the ML arising from mixing (e.g. owing to upwelling, wind- or convection-induced overturning or entrainment), and Δt represents the duration of the episodic mixing event. The specific values of κ would depend on the intensity of the mixing event, strength of stratification and vertical shear at the base of the ML. We do not expect κ to be uniform in time and space, but by choosing a constant value, we are assessing the response of surface pCO₂ to the same intensity of mixing or upwelling applied at any location. The value of Δt is representative of the duration of an episodic mixing event. A larger (or smaller) value of κ or Δt would simply result in an equivalently larger (or smaller) response that can be linearly scaled from the results presented.

The relative pCO₂ change owing to mixing is estimated globally using the monthly climatological datasets as the sum of various contributions. The physical effects of vertically mixing T, DIC, ALK and S are cumulatively termed the 'abiotic' response, in contrast to the biological response arising from the consumption of DIC in Redfield proportion to the vertically fluxed NO₃. The increase in alkalinity arising from any excess (unconsumed) NO₃ is also included in the biological response, but is negligible. The effect of salinity perturbations on pCO₂ is negligible compared with the other factors and is not discussed further or presented separately.

Before presenting our results, we assess their sensitivity to variations in the MLD. Recomputing the effect of mixing on the relative change in surface pCO₂ with the climatological MLD altered by ±20 per cent reveals very little sensitivity to a relative change in the MLD. MLD variations are significant only when the ML is shallow (less than 50 m in summer). At such times, perturbations in MLD that exceed 10 m are large (greater than 20%) in relative terms and can affect the response.

4. Results

(a) Varied response of surface pCO₂ to mixing

The net response of surface pCO₂ to vertical mixing is highly variable in space and time. Figure 1a,b shows global maps of the relative change in surface pCO₂ arising from mixing (equation (2.5)) during January and July. Mixing of the same intensity ($\kappa = 10^{-3}\,\mathrm{m^2\,s^{-1}}$) and duration ($\Delta t = 1$ day) is applied globally at the base of the ML to make this assessment. Warm colours (yellow and reds) indicate regions where vertical mixing would enhance the surface pCO₂, whereas cool colours indicate where pCO₂ would be lowered. Large areas of the ocean (coloured in grey or in light shades) show little sensitivity to vertical mixing. While some regions indicate an increase in pCO₂ owing to vertical fluxes, others would experience a decrease. Sensitivity to vertical mixing becomes enhanced in stratified regions; hence a much larger response is seen in the hemisphere experiencing summer. This single factor of summertime stratification gives rise to a large seasonality in the response of surface pCO₂. A large response is also
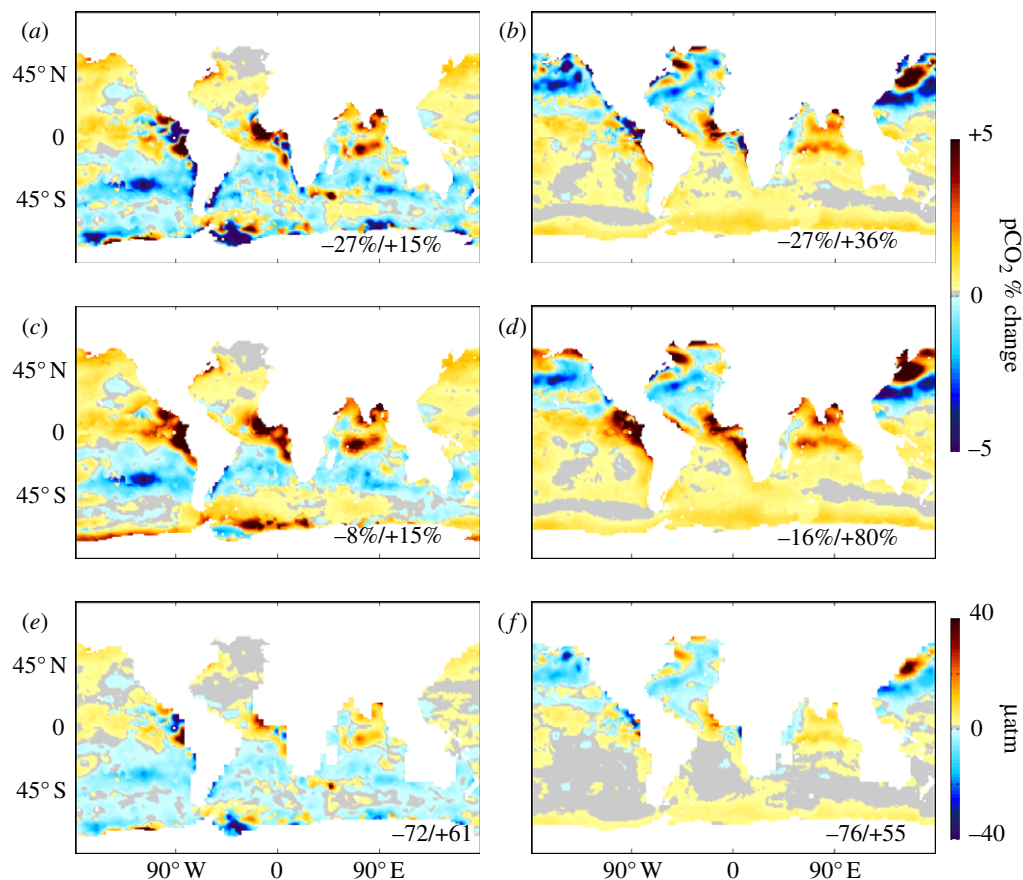
Figure 1. Left and right columns contrast results for January and July. (a,b) Net relative change in surface pCO_2 owing to the sum of various effects in January and July, respectively. (c,d) Relative change in pCO_2 owing to abiotic effects, i.e. without taking into account BIO, the uptake of DIC by phytoplankton production supported by a NO_3 flux. (e,f) Net change in pCO_2 (resulting from all effects) in response to vertical mixing, based on the climatological monthly surface pCO_2 [4]. The ABIO (abiotic) effect is the sum of T, DIC, ALK and S effects, whereas the net effect comprises the ABIO and BIO effects. (Online version in colour.)

found on the eastern upwelling margins of the ocean basins. Though we use a colour bar between ± 5 per cent, the maximum range (for the chosen value of mixing) extends from -27 to $+36$ per cent. This range, extending from negative to positive, indicates that the same mixing event acting in different locations could elicit a completely opposite response. In some regions, contrasting or opposite tendencies are seen to occur in close proximity of one another. For example, on either side of the Kuroshio and Gulf Stream, and along the eastern equatorial margins, we see alternating positive and negative responses on opposite sides of a front.

Figure 1c,d shows the net abiotic response in surface pCO_2. Here, the effects of biological consumption are not included. Comparison with the panels above (showing the net effect with biological uptake) reveals that in most regions,

biological uptake does not have a dominant role in modifying the pCO_2 response on these scales. This is with the exception of some high-latitude regions in summer, but the results are not reliable in the Southern Ocean, where NO_3 is known to remain unconsumed in the surface ocean. When estimating the biological contribution, no time lag is considered and the biological uptake is assumed to be NO_3 limited.

To estimate the absolute change in surface pCO_2 that would result from such perturbations, we multiply the relative change in pCO_2 by the monthly, climatological surface pCO_2 [4]. The resulting patterns in surface pCO_2 variation (figure 1e,f) are similar to the relative pCO_2 change (figure 1a,b), and show little or no similarity to the monthly pCO_2 distribution [4]. This suggests that the pCO_2 response to vertical mixing is governed by the subsurface gradients in the various properties, and not by the value of the surface pCO_2 *per se*. The largest variations in surface pCO_2 occur in the eastern upwelling regions and western boundary currents, and are in the range of -75 to $+60\,\mu$atm for the chosen strength of mixing.

(b) Effects of individual properties

To tease apart the contribution of individual factors to the relative change in surface pCO_2, we plot each of the terms in equation (2.5). These are referred to as the T effect $= (-\kappa\Delta t/H)(\beta\partial\mathrm{T}/\partial z)$, DIC effect $= (-\kappa\Delta t/H)$ $((\xi/\mathrm{DIC})(\partial\mathrm{DIC}/\partial z))$, ALK effect $= (-\kappa\Delta t/H)((\xi_A/\mathrm{ALK})(\partial\mathrm{ALK}/\partial z))$ and BIO effect $= S_{\mathrm{DIC}}$ (equation (2.6)). The contributions of salinity and S_{ALK} are small and are not shown. Figure 2 shows global maps of the remaining factors in January and July. The effect of DIC is opposite to that of T. While the entrainment of cooler water from subsurface lowers surface pCO_2 (indicated by blue shades in figure 2a,b), the consequent enhancement in surface DIC increases surface pCO_2, and is consequently shown in yellow and red colours (figure 2c,d). A vertical flux of ALK from the subsurface can either increase or decrease the surface pCO_2 according to whether the vertical gradient in ALK is positive or negative (figure 2e,f). The vertical supply of NO_3 results in an uptake of DIC (lowering pCO_2 as indicated in blue; figure 2g,h), which offsets some of the DIC fluxed into the ML. Grey regions indicate a lack of sensitivity of surface pCO_2 to upwelling. The examination of individual factors explains why one might see a large change in pCO_2 owing to upwelling at certain locations, but not at others.

Among the various factors, DIC, T and BIO can make a maximum contribution of about 25 per cent in certain regions, whereas ALK has a smaller range of approximately ± 10 per cent. We would expect the BIO effect to be generally negative as NO_3 increases with depth and mixing causes an enhancement of NO_3 and consumption of DIC in the ML. But the use of an average value over the ML can sometimes cause an unphysical reversal of gradient at the base, giving rise to a weak-positive BIO effect in some regions.

Figure 2 indicates that the surface pCO_2 is most responsive to upwelling in the western boundary systems and coastal upwelling zones. South of the Gulf Stream and Kuroshio temperature has a controlling effect on pCO_2 variations, such that surface pCO_2 would be lowered in response to upwelling. North of the Gulf Stream and Kuroshio, DIC has a dominant effect and pCO_2 would increase in response to upwelling. The upwelling region off the west coast of Central America also shows
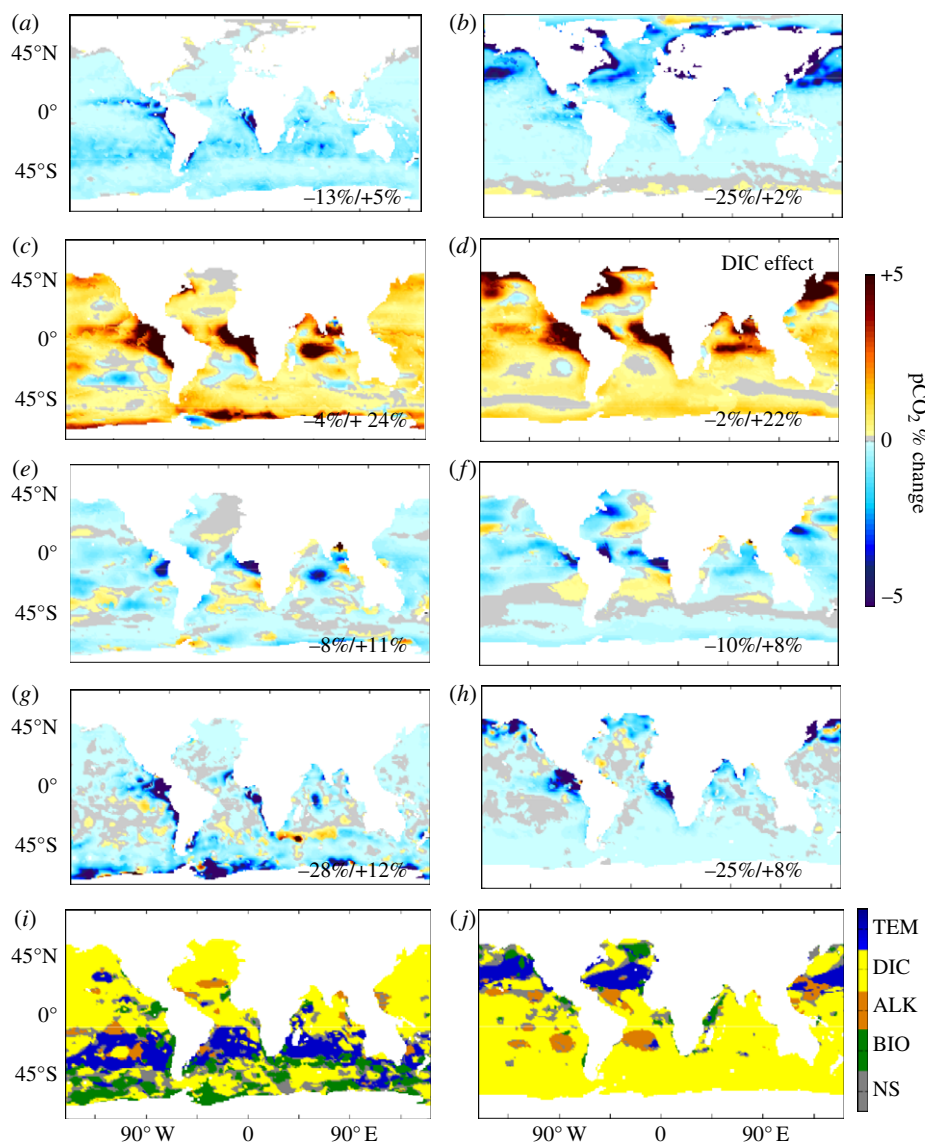
Figure 2. Percent change in surface pCO$_2$ in response to localized vertical mixing separated in to various factors: (a,b) T, (c,d) DIC, (e,f) ALK, (g,h) BIO, i.e. biological uptake owing to inputs of NO$_3$. For $(a–h)$, the range of results is presented in the lower right section of each panel. The lowermost panels (i,j) indicate which of these factors has the largest influence on surface pCO$_2$; 'NS' indicates the factor is not significant because it is over-run by opposing influences. These effects are estimated for January (a,c,e,g,i) and July (b,d,f,h,j). Effects of T and BIO would lower surface pCO$_2$, whereas DIC would enhance surface pCO$_2$. ALK may have either sign. Each of the effects becomes stronger in regions experiencing summer. These estimates are for a vertical diffusivity of $10^{-3}\,\mathrm{m^2\,s^{-1}}$ acting at the base of the ML for a day, but stronger/weaker mixing would result in a proportionally higher/lower perturbation in pCO$_2$. (Online version in colour.)

alternating positive and negative perturbations along the coast, with a dominance of the DIC effect off Chile, dominance of the BIO effect off the Peruvian upwelling zone, and DIC dominance further north towards Baja California.

Our results suggest that the response of surface pCO_2 to mixing varies regionally and temporally. Various effects can dominate the pCO_2 perturbation. Figure 2*i,j* indicates which effect dominates in a given region during January and July. If the dominant effect does not control the surface pCO_2 variation (i.e. if the response is opposite in sign), we leave the region grey. Since the effects of ALK and salinity are relatively small, the surface pCO_2 is, in general, lowered by upwelling when the effect of T plus biology (BIO) exceeds the effect of upwelled DIC. In most regions of the ocean, the effect of DIC dominates, although BIO and T effects do exceed the DIC effect in certain regions. In regions where the T or BIO effect dominates, pCO_2 will be lowered owing to vertical fluxes (assuming the ALK effect is small).

(c) Seasonally varying response at specific sites

To examine the processes responsible for the seasonal changes in pCO_2 owing to localized mixing more closely, figure 3 presents monthly results for four specific sites, namely the Joint Global Ocean Flux Study (JGOFS) sites of the Bermuda Atlantic Time Series (BATS) and Hawaii Ocean Time series (HOT), as well as the North Atlantic Bloom Experiment (NABE site at 47° N) and the Antarctic Polar Frontal Zone (APFZ) site. In general, the largest potential changes in pCO_2 arising from localized mixing events occur in the summer, when the ML is shallowest and the gradients at its base are sharpest. In the wintertime, deep MLs result in a relatively homogeneous water column and the impacts of mixing are thus minimized. Nevertheless, it is also important to note that the degree of density stratification is greatest during the summer, which may make it more difficult to obtain a large vertical flux.

If we first examine the subtropical stations BATS and HOT, we find that although the DIC effect consistently increases pCO_2 year round (figure 3), the impact of temperature is different between the two sites. The T effect contributes a large reduction in pCO_2 during the summertime at BATS, whereas it makes virtually no contribution at HOT. This is because the thermocline is much sharper and shallower at BATS relative to HOT (for example, between 0 and 100 m, figure 3), which leads to a greater cooling of surface waters and hence a reduction in pCO_2 in response to localized mixing. The impact of biological production at both sites is of little consequence, because the nitricline is consistently deeper than the ML (i.e. the depth across which anomalous mixing occurs, figure 3). Accordingly, at BATS, the T effect (and to a lesser extent the ALK effect) can more than offset the increased pCO_2 owing to the DIC effect in summer and mixing contributes to a net reduction in pCO_2 between May and August. At HOT, the T effect is too weak to counterbalance the DIC effect and mixing results in a small relative increase in pCO_2.

At the high-latitude stations (NABE and APFZ), there is a great deal of seasonality. At NABE, mixing has little impact during the winter, since MLs are already very deep (greater than 200 m). In the spring and summer, mixing of DIC increases pCO_2 greatly and the counterbalancing effect of temperature is not as large as at BATS. Hence, the net effect of all abiotic processes results
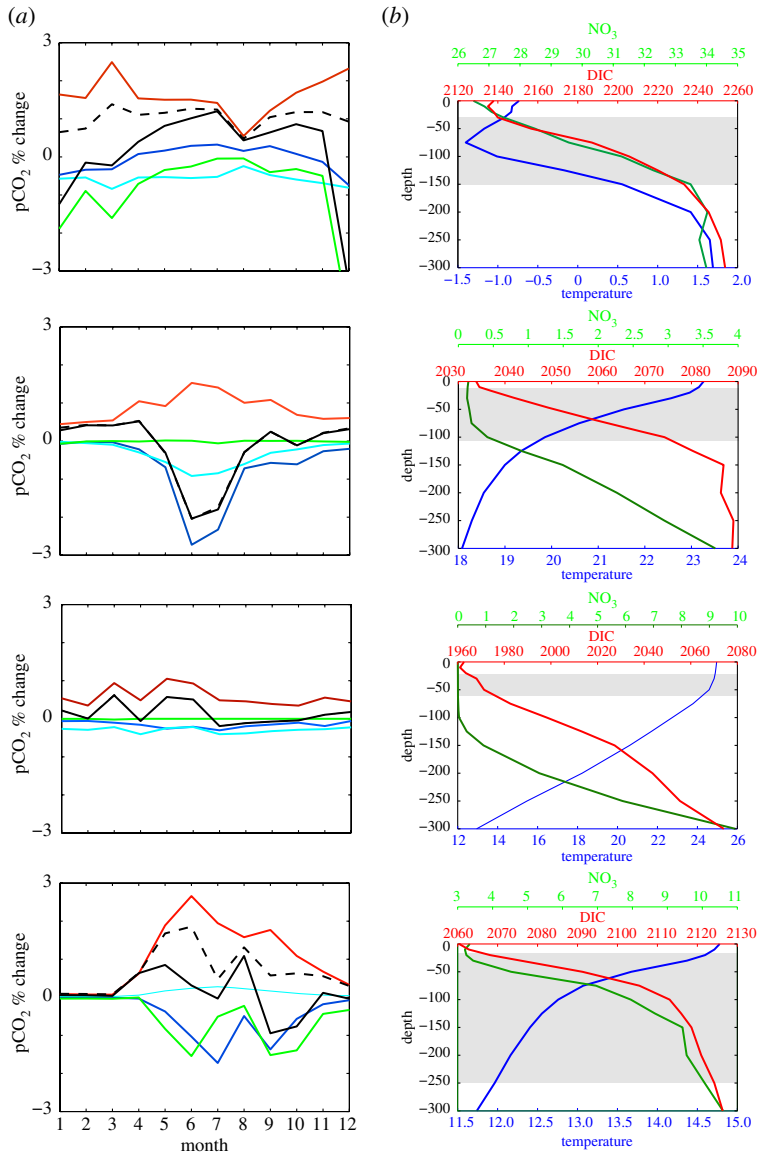
Figure 3. The results are contrasted among various oceanic regions through time series and profiles averaged over a $5° \times 5°$ region centred on the Antarctic Polar Frontal Zone (APFZ at $65°$ S, $170°$ W), Bermuda Atlantic Time Series (BATS at $32°$ N, $64°$ W), Hawaii Ocean Time series (HOT at $23°$ N, $158°$ W) and the site of the North Atlantic Bloom Experiment (NABE at $47°$ N, $20°$ W). (*a*) Annual monthly time series showing the relative change in surface pCO_2 arising from the upwelling/mixing related effects of T, DIC, ALK, BIO, the total abiotic component ABIO, and the net sum of all effects. Positive/negative values indicate the potential for a relative increase/decrease in surface pCO_2, owing to mixing represented by $\kappa = 10^{-3}\,\mathrm{m\,s^{-2}}$ acting at the base of the ML for 1 day. (*b*) Annual mean vertical profiles of temperature (°C), DIC (μmol l^{-1}) and NO$_3$ (μmol l^{-1}) at the same sites from climatological data. The range in MLD over the annual cycle is shaded grey. Dark blue line, T; red line, DIC; sky blue line, ALK; green line, BIO; dash-dotted line, ABIOTIC; black line, total. (Online version in colour.)

in a net increase in pCO_2 in response to localized mixing between March and November (figure 3). However, the biological effect during the spring to autumn period is much larger than at BATS or HOT, because the nitricline is much shallower, and is thus almost able to offset the net effect of abiotic processes for much of the spring and summer. Including the impact of biology means that mixing actually leads to a net reduction in pCO_2 during September and October (figure 3). However, it is important to note that biology needs to act in concert with T to drive the reduction in pCO_2 during this period. The APFZ similarly shows large changes throughout the year. As seen previously, mixing of DIC causes large increases in pCO_2 even in the winter (as winter MLs are shallower than at NABE). This is offset slightly by the combination of the smaller effects of T and ALK during the spring and summer, but still results in a net increase in pCO_2 owing to abiotic processes. Localized mixing causes a large net reduction in pCO_2 between November and March. This is due to a large increase in biological productivity associated with the increased vertical flux of NO_3 that can more than counterbalance the net increase in pCO_2 associated with abiotic processes. However, the BIO effect might be overestimated in the iron-limited APFZ, if the ferricline were deeper than the nitricline. The biological response to a localized mixing event is based on the NO_3 profile and assumes a fixed C/N ratio. However, increasing the supply of iron to phytoplankton results in a concomitant increase in their demand for iron [25,38]. This would be translated into a reduction in the C/Fe ratio in response to an increased vertical flux of iron associated with a localized mixing event. As such, our results regarding the biological response should be seen as maximal effects in the iron-limited Southern Ocean.

Overall, we find that there are often compensatory processes that act in concert to moderate or enhance the response of surface pCO_2 to localized mixing on a month by month basis. While DIC always drives an increase in surface pCO_2, T and/or BIO are able to compensate for this effect during the summertime and cause a net reduction in pCO_2 at some stations. Biology is generally weak in the tropics and T can cause a seasonal reduction in pCO_2 at BATS, but not at HOT. This is due to variability in the thermocline depth, relative to the depth of mixing between each station. On the other hand, the T effect is weaker at high latitudes (NABE and APFZ) and biological activity is the predominant means by which the impact of DIC is offset to cause a net pCO_2 reduction in summer. The combination of T and BIO is more important at NABE than at APFZ, although we note that the BIO effect might be overestimated at APFZ.

5. Discussion

The proposed framework allows us to synthesize the findings of several recent studies that have examined the response of the surface ocean to upwelling or mixing events. Bates *et al.* [15] found that in the Sargasso Sea, the surface ocean cooled by several degrees with the passing of hurricane Felix in 1995. The lowered temperature affected the surface pCO_2, which was lowered by 60 µatm. A similar effect was reported by Koch *et al.* [39]. This is consistent with our analysis (figure 2*b*), which shows that in the region of the Sargasso Sea, the effect of temperature (T effect) dominates the change in surface pCO_2 induced by mixing

during summer. Further to the north (at 72.5° W, 39.5° N), the passage of extra-tropical hurricane Gustav (in 2002) caused no significant cooling, but an increase in sea surface pCO_2 of 50 µatm owing to the enhancement of DIC [24]. This too is consistent with figures 1 and 2, which show the dominance of the DIC effect and potential increase in pCO_2 owing to mixing in this region over the summer.

Modelling studies that were based on conditions in the North Atlantic during the summer [22], as well as winter [23], revealed that upwelling induced by fronts and eddies generates little or no change in the surface pCO_2. This is consistent with our results, as we find that the change in pCO_2 in the northeast Atlantic is negligible in January (figure 1a) and less than 5 µatm in July, largely because the effects of lowered T and increased DIC negate each other. The largest changes in the North Atlantic are actually found on the western side, north of the Gulf Stream in January and on either side of the Gulf Stream in July, owing to stronger DIC gradients. However, the impact of vertical fluxes is not limited to one dimension. Modelling studies [22,23] have revealed that lateral stirring by mesoscale eddies of surface water masses with substantially different pCO_2 generates strong horizontal variability in surface pCO_2, as in observations [40]. This effect, not considered here, mainly redistributes pCO_2 variability to small spatial scales without significantly modifying its mean value, unlike the case where vertical fluxes are involved.

There are some important implications for the response of surface pCO_2 to episodic vertical fluxes. Regions and times that show a large sensitivity of surface pCO_2 to vertical mixing can be expected to exhibit greater spatial and temporal variance in surface pCO_2, which has consequences for calculating carbon budgets [41]. Secondly, changes in pCO_2 are concomitant with a change in seawater pH, or ocean acidification. Thus, this analysis helps to identify regions that would be particularly vulnerable to changes in pH, such as the west coast of North America where marine ecosystems could be at stake [42]. On the other hand, we expect that the impact of mixing-induced perturbations in surface pCO_2 on large-scale air–sea CO_2 fluxes would be negligible owing to the limited area and duration of the pCO_2 modulations [3]. In some instances, however, as in the case of hurricanes, a systematic correlation with higher wind speeds and gas exchange rates could enhance the sea-to-air gas flux as reported by Bates *et al.* [15].

Estimates of the BIO effect in this framework should be viewed with some caution. Our present results indicate that the effect of DIC broadly dominates the pCO_2 perturbation, and that vertically fluxed NO_3 does not account for the complete consumption (in Redfield proportion) of vertically fluxed DIC. In reality, the biological response to the vertical flux of nutrients is complex, depending on species composition, micro nutrients, variable stoichiometric ratios and variability in PAR. Thus, it is often difficult to capture the biological response even with ecosystem models, and the simplistic approach taken here may very well underestimate the biological contribution. Furthermore, we point out the potential for inconsistencies among the datasets used in this study since they are constructed from varied sources of data with different methods.

In the future, with climate change, we would expect an increase in surface ocean temperatures and vertical gradients in temperature. Consequently, the negative perturbation of T on pCO_2 owing to mixing (T effect) would be enhanced, even as surface pCO_2 is likely to be higher owing to higher surface T and DIC. Increasing surface DIC owing to the uptake of anthropogenic CO_2 will reduce the positive

effect of DIC on surface pCO_2 in response to mixing. Using the GLODAP data, we can estimate that the vertical gradient in DIC (between the surface and depths of 100–300 m) has already declined by 5–10% since the pre-industrial. Thus, the net effect is likely to be a reduction in the dominance of the DIC effect and increase in the dominance of the T effect, tending to decrease the surface pCO_2 perturbation (or make it more negative) in response to mixing. However, the effects of subduction and circulation are known to complicate this simple picture by sequestering more anthropogenic CO_2 at depth than at the surface in some locations. It is also likely that climate change will modify the degree of stratification [43], which may impact the strength and the frequency of episodic mixing events in the future.

6. Conclusions

We propose an analytical framework that we apply to observational datasets for analysing the impact of vertical fluxes in DIC, ALK, T, S and NO_3 on sea-surface pCO_2. We make a global, monthly, assessment of the surface pCO_2 perturbations owing to episodic mixing of a given strength. We find a great deal of spatial and temporal variability in the pCO_2 response at the sea surface, with the amplitude of the perturbation exceeding 20 µatm in many regions, and being positive in some areas and negative in others. The largest surface pCO_2 response to vertical mixing is found in eastern upwelling margins and regions with shallow MLs during the summer. The response depends on the interactive effects of DIC, T, ALK and biology, which can compensate or reinforce their individual effects. This explains why a given mixing event (e.g. the passage of a hurricane or vertical advection from frontogenesis) can elicit an increase or a decrease in surface pCO_2 depending on its precise location and timing. In general, entrainment of DIC from the subsurface increases surface pCO_2, while a reduction in T and the biological uptake of DIC act to reduce pCO_2. The response owing to ALK is spatially variable. In the future, climate change will probably modify the oceanic mean vertical gradients of temperature and DIC owing to the uptake of anthropogenic CO_2, thereby reducing pCO_2 perturbations and variability arising from vertical mixing, even as the mean surface pCO_2 may be higher.

References

1 Le Quéré, C. *et al.* 2009 Trends in the sources and sinks of carbon dioxide. *Nat. Geosci.* **2**, 831–836. (doi:10.1038/ngeo689)

2 Wanninkhof, R. 1992 Relationship between wind speed and gas exchange over the ocean. *J. Geophys. Res.* **97**, 7373–7382. (doi:10.1029/92JC00188)

3 Lenton, A., Matear, R. & Tilbrook, B. 2006 Design of an observational strategy for quantifying the Southern Ocean uptake of CO_2. *Global Biogeochem. Cyc.* **20**, GB40110. (doi:10.1029/2005GB002620)

4 Takahashi, T. *et al.* 2009 Climatological mean and decadal change in surface ocean pCO_2, and net sea–air CO_2 flux over the global oceans. *Deep Sea Res. II* **56**, 554–577. (doi:10.1016/j.dsr2.2008.12.009)

5 Archer, D., Takahashi, T., Sutherland, S., Goddard, J., Chipman, D., Rodgers, K. & Ogura, H. 1996 Daily, seasonal and interannual variability of sea-surface carbon and nutrient concentration in the equatorial Pacific Ocean. *Deep Sea Res. II* **43**, 779–808. (doi:10.1016/0967-0645(96)00017-3)

6 DeGrandpre, M., Hammar, T., Wallace, D. & Wirick, C. 1997 Simultaneous mooring-based measurements of seawater CO_2 and O_2 off Cape Hatteras, North Carolina. *Limnol. Oceanogr.* **42**, 21–28. (doi:10.4319/lo.1997.42.1.0021)

7 Borges, A. & Frankignoulle, M. 2001 Short-term variations of the partial pressure of CO_2 in surface waters of the Galician upwelling system. *Prog. Oceanogr.* **51**, 283–302. (doi:10.1016/S0079-6611(01)00071-4)

8 Copin-Montégut, C., Bégovic, M. & Merlivat, L. 2004 Variability of the partial pressure of CO_2 on diel to annual time scales in the northwestern Mediterranean Sea. *Mar. Chem.* **85**, 169–189. (doi:10.1016/j.marchem.2003.10.005)

9 Körtzinger, A., Send, U., Lampitt, R., Hartman, S., Wallace, D., Karstensen, J., Villagarcia, M., Llinás, O. & DeGrandpre, M. 2008 The seasonal pCO_2 cycle at 49°N 16.5°W in the northeastern Atlantic Ocean and what it tells us about biological productivity. *J. Geophys. Res.* **113**, C04020. (doi:10.1029/2007JC004347)

10 Leinweber, A., Gruber, N., Frenzel, H., Friederich, G. & Chavez, F. 2009 Diurnal carbon cycling in the surface ocean and lower atmosphere of Santa Monica Bay, California. *Geophys. Res. Lett.* **36**, L08601. (doi:10.1029/2008GL037018)

11 Merlivat, L., Davila, M. G., Caniaux, G., Boutin, J. & Reverdin, G. 2009 Mesoscale and diel to monthly variability of CO_2 and carbon fluxes at the ocean surface in the northeastern Atlantic. *J. Geophys. Res.* **114**, C03010. (doi:10.1029/2007JC004657)

12 Pollard, R. & Regier, L. 1992 Vorticity and vertical circulation at an ocean front. *J. Phys. Oceanogr.* **22**, 609–625. (doi:10.1175/1520-0485(1992)022<0609:VAVCAA>2.0.CO;2)

13 Klein, P., Hua, B. L., Lapeyre, G., Capet, X., Le Gentil, S. & Sasaki, H. 2008 Upper ocean turbulence from high-resolution 3-D simulations. *J. Phys. Oceanogr.* **38**, 1748–1763. (doi:10.1175/2007JPO3773.1)

14 Hales, B., Takahashi, T. & Bandstra, L. 2005 Atmospheric CO_2 uptake by a coastal upwelling system. *Global Biogeochem. Cyc.* **19**, GB1009. (doi:10.1029/2004GB002295)

15 Bates, N., Knap, A. & Michaels, A. 1998 Contribution of hurricanes to local and global estimates of air–sea exchange of CO_2. *Nature* **395**, 58–61. (doi:10.1038/25703)

16 Lovelock, J. & Rapley, C. G. 2007 Ocean pipes could help the Earth to cure itself. *Nature* **447**, 403. (doi:10.1038/449403a)

17 Klein, P. & Coste, B. 1984 Effects of wind-stress variability on nutrient transport into the mixed layer. *Deep Sea Res. A* **31**, 21–37. (doi:10.1016/0198-0149(84)90070-0)

18 McGillicuddy Jr, D., Robinson, A., Siegel, D., Jannasch, H., Johnson, R., Dickey, T., McNeil, J., Michaels, A. & Knap, A. 1998 Influence of mesoscale eddies on new production in the Sargasso Sea. *Nature* **394**, 263–266. (doi:10.1038/28367)

19 Mahadevan, A. & Archer, D. 2000 Modeling the impact of fronts and mesoscale circulation on the nutrient supply and biogeochemistry of the upper ocean. *J. Geophys. Res.* **105**, 1209–1225. (doi:10.1029/1999JC900216)

20 Lévy, M., Klein, P. & Treguier, A. M. 2001 Impacts of sub-mesoscale physics on production and subduction of phytoplankton in an oligotrophic regime. *J. Mar. Res.* **59**, 535–565. (doi:10.1357/002224001762842181)

21 Lévy, M., Klein, P. & Jelloul, M. B. 2009 New production stimulated by high-frequency winds in a turbulent mesoscale eddy field. *Geophys. Res. Lett.* **36**, L16603. (doi:10.1029/2009GL039490)

22 Mahadevan, A., Lévy, M. & Mémery, L. 2004 Mesoscale variability of sea surface pCO_2: what does it respond to? *Global Biogeochem. Cyc.* **18**, GB101710. (doi:1029/2003GB002102)

23 Resplandy, L., Lévy, M., d'Ovidio, F. & Merlivat, L. 2009 Impact of submesoscale variability in estimating the air-sea CO_2 exchange: results from a model study of the POMME experiment. *Global Biogeochem. Cyc.* **23**, GB1017. (doi:10.1029/2008GB003239)

24 Perrie, W., Zhang, W., Ren, X., Long, Z. & Hare, J. 2004 The role of midlatitude storms on air-sea exchange of CO_2. *Geophys. Res. Lett.* **31**, L09306. (doi:10.1029/2003GL019212)

25 Dutreuil, S., Bopp, L. & Tagliabue, A. 2009 Impact of enhanced vertical mixing on marine biogeochemistry: lessons for geo-engineering and natural variability. *Biogeosciences* **6**, 901–912. (doi:10.5194/bg-6-901-2009)

26 Yool, A., Shepherd, J., Bryden, H. & Oschlies, A. 2009 Low efficiency of nutrient translocation for enhancing oceanic uptake of carbon dioxide. *J. Geophys. Res.* **114**, C08009. (doi:10.1029/2008JC004792)

27 Locarnini, R., Mishonov, A., Antonov, J., Boyer, T. & Garcia, H. 2006 World Ocean Atlas 2005, vol. 1: temperature. Technical report, NOAA Atlas NESDIS 61, US Government Printing Office, Washington, DC.

28 Antonov, J., Locarnini, R., Boyer, T., Mishonov, A. & Garcia, H. 2006 World Ocean Atlas 2005, vol. 2: salinity. Technical report, NOAA Atlas NESDIS 62, US Government Printing Office, Washington, DC.

29 Garcia, H. E., Locarnini, R. A., Boyer, T. P. & Antonov, J. 2006 World Ocean Atlas 2005, vol. 4: nutrients (phosphate, nitrate, silicate). Technical report, NOAA Atlas NESDIS 64, US Government Printing Office, Washington, DC.

30 Key, R. *et al.* 2004 A global ocean carbon climatology: results from GLODAP. *Global Biogeochem. Cyc.* **18**, GB4031. (doi:10.1029/2004GB002247)

31 Takahashi, T., Olafsson, J., Goddard, J., Chipman, D. & Sutherland, S. C. 1993 Seasonal variation of CO_2 and nutrients in the high-latitude surface oceans: a comparative study. *Global Biogeochem. Cyc.* **7**, 843–878. (doi:10.1029/93GB02263)

32 Sarmiento, J. & Gruber, N. 2006 *Ocean biogeochemical dynamics*. Princeton, NJ: Princeton University Press.

33 de Boyer Montégut, C., Madec, G., Fischer, A., Lazar, A. & Iudicone, D. 2004 Mixed layer depth over the global ocean: an examination of profile data and a profile-based climatology. *J. Geophys. Res.* **109**, C12003. (doi:10.1029/2004JC002378)

34 Lenton, A., Metzl, N., Takahashi, T., Sutherland, S., Tilbrook, B., Kuchinke, M. & Sweeney, C. Submitted. The observed evolution of the trends and drivers of oceanic pCO_2 over the last two decades.

35 Walsh, J. 1978 A data set on northern hemisphere sea ice extent, 1953–1976. Technical report GD-2, 49-51, World Data Center for Glaciology (Snow and Ice), Boulder, CO.

36 Zwally, H., Comiso, J., Parkinson, C., Campbell, W., Carsey, F. & Gloerson, P. 1983 Antarctic sea ice, 1973–1976: satellite passive microwave observations. Technical report. ADA278193, NASA, Washington, DC.

37 Lengaigne, M., Madec, G., Bopp, L., Menkes, C., Aumont, O. & Cadule, P. 2009 Bio-physical feedbacks in the Arctic Ocean using an earth system model. *Geophys. Res. Lett.* **36**, L21602. (doi:10.1029/2009GL040145)

38 Sunda, W. & Huntsman, S. 1997 Interrelated influence of iron, light and cell size on marine phytoplankton growth. *Nature* **390**, 389–392. (doi:10.1038/37093)

39 Koch, J., McKinley, G., Bennington, V. & Ullman, D. 2009 Do hurricanes cause significant interannual variability in the air-sea CO_2 flux of the subtropical North Atlantic? *Geophys. Res. Lett.* **36**, L07606. (doi:10.1029/2009GL037553)

40 Watson, A., Robinson, C., Robinson, J., Williams, P. & Fasham, M. 1991 Spatial variability in the sink for atmospheric carbon dioxide in the North Atlantic. *Nature* **350**, 50–53. (doi:10.1038/350050a0)

41 Monteiro, P. *et al.* 2009 A global sea surface carbon observing system: assessment of changing sea surface CO_2 and air-sea CO_2 fluxes. Technical report, OceanObs Community White Paper, Venice, Italy.

42 Feely, R. *et al.* 2008 Evidence for upwelling of corrosive 'acidified' water onto the continental shelf. *Science* **320**, 1490–1492. (doi:10.1126/science.1155676)

43 Sarmiento, J. *et al.* 2004 Response of ocean ecosystems to climate warming. *Global Biogeochem. Cyc.* **18**, GB3003. (doi:10.1029/2003GB002134)